JOURNAL OF CATALYSIS **150**, 186–198 (1994)

Transformation of Platinum into a Stable, High-Temperature, Dehydrogenation–Hydrogenation Catalyst by Ensemble Size Reduction with Rhenium and Sulfur

F. H. Ribeiro,* A. L. Bonivardi, C. Kim,[1] and G. A. Somorjai[2]

*Department of Chemistry, University of California at Berkeley, Berkeley, California 94720; and *Center for Advanced Materials, Materials Sciences Division, Lawrence Berkeley Laboratory, Berkeley, California 94720*

Received January 24, 1994; revised July 5, 1994

The effect of the addition of rhenium and sulfur on the catalytic properties of platinum and on its ability to resist deactivation by carbonaceous deposits was studied. The reactions of neopentane (2,2-dimethylpropane), *n*-hexane, and cyclohexane in excess H_2 were studied on model bimetallic catalysts prepared by the deposition of platinum on a rhenium foil or vice versa. The rates were measured in a batch reactor with a ratio of H_2 to hydrocarbon of 30 or 60, a H_2 pressure of 450 kPa, and a reaction temperature in the range of 570 to 800 K. Rhenium–sulfur is catalytically inactive and acted only as a diluent to platinum. As the platinum ensembles on the surface became smaller by dilution with rhenium–sulfur, the rates of the structure-sensitive reactions decreased rapidly and eventually only hydrogenation–dehydrogenation reactions were observed. Most importantly, as the size of the platinum ensembles decreased, they became more resistant to poisoning than the larger ones. © 1994 Academic Press, Inc.

1. INTRODUCTION

The catalytic transformation, in the presence of hydrogen, of gasoline-range hydrocarbons of low octane number into hydrocarbons of high octane is an important and high-volume process in the petroleum industry referred to as catalytic reforming. The chemistry in the reforming of hydrocarbons involves two types of sites and for this reason it is called a bifunctional mechanism (see Ref. (1) for details on this process). The first type of sites (platinum) can catalyze hydrogenation–dehydrogenation reactions and the second type of sites (halogen-modified alumina) is one with enough acidity to catalyze skeletal isomerization of olefins. A typical industrial catalyst uses 0.3% Pt by weight (platinum area of about 0.5 $m^2\ g^{-1}$) on a high surface area (about 200 $m^2\ g^{-1}$) acidic alumina. The reason for the vast difference in surface area between the two sites is that the hydrogenation–dehydrogenation areal rates are much faster than the areal rates of isomerization of olefins, and in fact the latter reaction is the rate-determining step (2). The chemistry involved in the reforming process can be illustrated by the formation of benzene from *n*-hexane (3). *n*-Hexane is first dehydrogenated to 1-hexene over platinum, which is cyclized to methylcyclopentane on an acid site (4). Methylcyclopentane is then dehydrogenated into methylcyclopentene which is isomerized on an acid site to cyclohexene (4, 5). Finally, cyclohexene is further dehydrogenated to benzene over platinum.

In addition to hydrogenation–dehydrogenation, platinum itself can catalyze other reactions in the presence of H_2 (6). For example, on a *n*-hexane feed platinum can catalyze the formation of 2- and 3-methylpentane (isomerization), methylcyclopentane (cyclization), benzene (dehydrocyclization), and smaller hydrocarbons (hydrogenolysis) (7). Under conditions employed in reforming reactions, a given product will be formed through a monofunctional (platinum) or bifunctional mechanism depending on the catalyst composition and reaction conditions. The reactions that can be catalyzed by platinum have different requirements on the number of contiguous platinum atoms. The hydrogenolysis and dehydrocyclization reactions are the more demanding in number of sites followed by the reactions of isomerization and cyclization and finally the hydrogenation–dehydrogenation reactions which probably require only one platinum atom (8). Thus, depending on how many contiguous sites are present on the platinum surface a difference in the product distribution will be seen.

The reforming process has been carried out mostly by platinum catalysts supported on acidic supports since 1950 and more recently (1967) by the addition of a second metal to the supported platinum catalyst (9). The advantage of bimetallic catalysts (10) is that they are more resistant to catalyst deactivation, which occurs primarily by

---

[1] Present address: Department of Chemistry, Kyungpook National University, Taegu, 702-701, Korea.

[2] To whom correspondence should be addressed.

0021-9517/94 $6.00

the formation of carbonaceous deposits on the catalyst through undesired parallel reactions (11). This higher resistance translates into longer operation before regeneration of the catalyst is required or a similar life span but the possibility of running at reaction conditions (higher temperature, lower H_2 pressure) that permit a higher product octane. The bimetallic catalysts in current use are Pt–Re, Pt–Sn, and Pt–Ir.

The first reforming bimetallic catalyst to be used in industrial operation was Pt–Re (12) and since that time a large effort has been made to explain the mode of operation of this catalyst. There are two features of this system that make the elucidation of the role of Re harder. The first is that the difference in the stability of the monometallic platinum and bimetallic platinum–rhenium catalyst can be detected only after many hours of operation thus making it difficult for research studies. The second is that the commercial system is composed of small amounts of Pt and Re (0.3% each) dispersed on a high surface area support which makes the preparation and identification of particular phases very difficult. One way to approach this complex problem is to work with model catalysts. This method is being used with supported catalysts (13) and on single crystals and foils (14). This approach has been successful using platinum single crystals with different crystallographic orientation (15, 16) and also in studies of the Pt–Re bimetallic system (17–19). The advantages of this system are that surface science techniques can be applied before and after reaction and that the reaction can be carried out at temperatures and pressures appropriate to industrial catalysts. The purpose of this paper was to employ this powerful technique to decide among the many mechanisms proposed in the literature for the mode of action of rhenium. Some of the proposed models include the stabilization of platinum by rhenium against sintering by anchoring (20), formation of stable, catalytically active, rhenium compounds by interaction with the alumina (21), alloying of Re with Pt (22), and interaction of the alloy with sulfur (23–28). The last mode of action proposes that sulfur binds primarily with rhenium forming a catalytically inactive rhenium–sulfur compound that partition the number of platinum sites. These smaller platinum ensembles are more difficult to poison because of steric hindrance from the protruding sulfur atoms that inhibits the growth of large islands of polymeric carbon that are difficult to rehydrogenate. In this paper, this model was verified by preparing platinum–rhenium–sulfur surfaces of different composition and testing them in the reactions of *n*-hexane and cyclohexane. The results in this paper support the contention that small ensembles of platinum are more resistant to deactivation than larger ones. By the presence of rhenium and sulfur all large ensembles of platinum are poisoned so that only hydrogenation–dehydrogenation activity of the metal remain. All other chemical changes are shifted onto the acid component of the catalyst.

2. EXPERIMENTAL METHODS

2.1. General Methods

The experiments were run on an ultrahigh vacuum (UHV) chamber with a base pressure of 1.0×10^{-7} Pa (7.5×10^{-10} Torr) and equipped with a containment cell capable of enclosing the sample and holding a pressure of about 2 MPa (20 atm). The containment cell was connected to an external loop containing a gas compressor (Whitey, LC-10) for the gas recirculation, forming a batch reactor with a total reactor volume of 460 cm^3. The flow rate in the reactor was estimated from the manufacture's charts to be about 15 $cm^3\ s^{-1}$. This flow rate permitted a conversion per pass of less than 0.02%. The UHV chamber was equipped with a retarding field analyzer AES with the electron beam at 1500 eV and hitting the sample at a grazing angle, a sputter Ar gun operating at 2000 eV, two leak valves, and an UTI quadrupole mass spectrometer. The chamber also contained a metal and sulfur deposition source to be described in more detail below. The sample was heated resistively and the temperature was measured through a thermocouple type K spot-welded on the center upper edge of the foil.

The catalysts used in this study were polycrystalline metal foils. The platinum foil was 0.076 mm thick with a total surface area of 0.5 to 1 cm^2 and with a purity of 99.95% (Lawrence Berkeley Laboratory pool stock). It was spot-welded to 0.51-mm-diameter platinum wires on two sides of the approximately square foil. The platinum wires protruded about 2 mm from the foil and were spot-welded to 0.71-mm-diameter gold wires which were extended to the copper sample manipulator where they were held into place by a set of screws. The rhenium foil was 0.1 mm thick, had a total surface area of 0.5 cm^2, and a purity of 99.99% (Johnson Matthey). The rhenium foil was spot-welded to two 0.71-mm stainless-steel 308 wires which extended directly to the copper sample manipulator.

Both sides of the platinum and rhenium foils were cleaned by cycles of Ar sputtering at room temperature, O_2 treatment at 1000 K and 4×10^{-9} Pa (5×10^{-7} Torr), and annealing at 1173 K until the AES spectra showed no foreign peaks. After each reaction studied, which involved the deposition of rhenium over the platinum foil or vice versa, Ar sputtering for 1 h on each side followed by annealing at 1173 K was sufficient (as shown by AES) to free the surface from the deposited metal.

The deposition of rhenium on the platinum foil or platinum on a rhenium foil, was accomplished by a metal vapor vacuum arc plasma (MEVVA) source. The operation and principle of this device has been described before (29).

In short, the cathode, which is made of the metal to be deposited, is biased by several hundred volts while the stainless steel anode is grounded. An arc discharge through the cathode–anode circuit forms a dense plasma plume of the material of the cathode. The arc discharge is started by a high voltage pulse on a trigger electrode. Because the arc discharge is precisely controlled, it is very easy to vary (by the number of pulses applied) and reproduce the metal coverage on a foil. A coverage from 7% to many monolayers were accomplished in this study. Figure 1 shows the amount of platinum or rhenium deposited as a function of the number of pulses applied.

The samples were presulfided to the saturation amount of sulfur in UHV by atomic sulfur generated from a solid-state electrochemical cell (Pt/Ag/AgI/Ag_2S/Pt) (30) before reaction.

The samples for reaction studies were prepared as follows. After cleaning and annealing, the desired amount of metal was deposited and the sample was immediately sulfided to the saturation coverage amount with atomic sulfur. The sample was then annealed at 1000 K for 1 min and sulfur was deposited again at room temperature to replenish any lost sulfur during the annealing treatment. Finally, the sample was heated to 800 K for 5 min with the sulfur source still on.

AES measurements were collected after reaction. The procedure to stop the reaction consisted of first switching off the heating current to the sample (it cooled to about 320 K in a few seconds) and then evacuating the cell at room temperature. An AES spectrum was taken as soon as the high-pressure cell was opened to the UHV environment. Interference from the large sulfur and carbon peaks in the spectrum with the rhenium and platinum peaks allowed analysis only in the region from 200 to 240 eV.

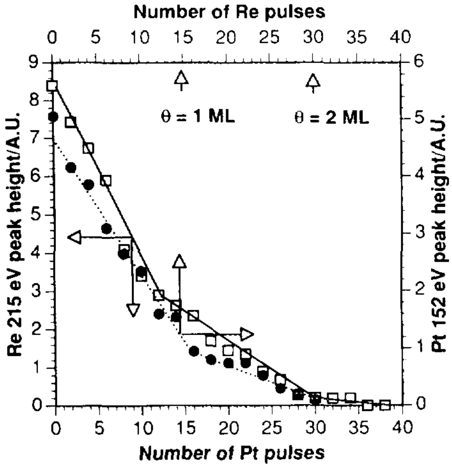

FIG. 1. Rhenium 215 eV (□) and Platinum 152 eV (●) AES peak height on a rhenium and on a platinum foil as a function of the number of platinum and rhenium pulses, respectively.

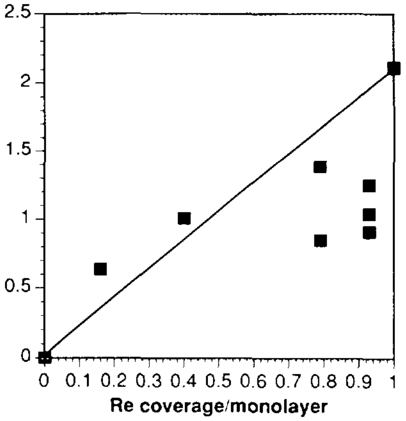

FIG. 2. Ratio of the AES Re 215 eV peak to the combined platinum and rhenium peak (Pt + Re 237 eV) as a function of rhenium coverage.

Taking into account the rhenium coverage determined independently from the AES measurements by the neopentane reaction (see Section 3.1.) and that the intensity of the rhenium 227 eV peak is about 2.3 times lower than the Pt 237 eV peak (31), it was found that the peak centered around 237 eV and composed of the Re 227 and Pt 237 eV (the peaks were not resolved) was approximately constant as the surface concentration of Re was varied. The combined Pt + Re 237 eV peak height was then used as a measure of the total amount of surface metal atoms, necessary to specify the relative coverage of sulfur and carbon. Figure 2 shows how the rhenium signal changes as a function of rhenium coverage on a platinum foil.

2.2. *Rate Measurement*

The reaction-rate measurements were made in a batch mode. The hydrocarbons *n*-hexane (Fluka, puriss), neopentane (Phillips, research grade, 99.8%) and cyclohexane (Fluka, puriss) were degassed by freeze–thaw cycles. The hydrocarbons were introduced before H_2 (Matheson, prepurified). Most of the experiments were run with 6.7 or 13.3 kPa (50 or 100 Torr) of hydrocarbon and 450 kPa (3300 Torr) of H_2. The reactant mixture was circulated for 20 min before the foil was heated to the reaction temperature. The reaction products were analyzed by a gas chromatograph (Hewlett-Packard 5890-II) with a flame ionization detector. The products were separated on a 50-m-long, 0.2-mm-diameter column (Pona). The first analysis was done after 3 min of reaction and subsequent analyses were carried out at intervals of 10–15 min. A typical accumulation versus time plot is shown in Fig. 3 for the reaction with neopentane. Although the number of turnovers is very high at the end of the experiments, the total conversion was only 0.8%, which accounts for the pseudo-zero order kinetics. The initial turnover rate was calculated from the slope of the lines shown. In this paper

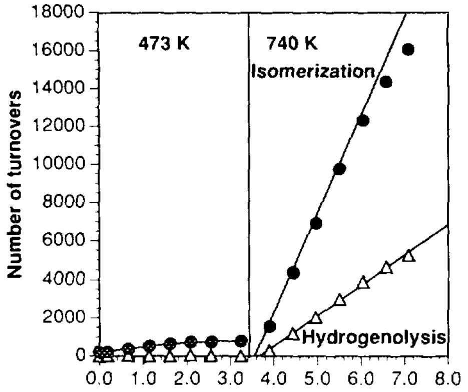

FIG. 3. Number of neopentane molecules converted to isopentane (●) and to hydrogenolysis products (△) per surface platinum atom as a function of time. Reaction run on a sulfided platinum foil at 13.3 kPa of neopentane and 450 kPa of H_2. The reaction temperature for the two runs is shown in Fig. 3.

the rates will be described as *nominal turnover rates* and as *turnover rates*. The nominal turnover rate includes all surface atoms (platinum and rhenium) as active sites while the turnover rate will include only the surface platinum atoms. An atom surface density of 1.0×10^{15} atoms cm^{-2} was used in the rate calculations.

On the *n*-hexane reactions, a second reaction was run to study the sample deactivation. The test procedure consisted of cooling the sample after the first run under the reaction mixture, evacuating it at room temperature, and recharging the reactants to the reactor. The same procedure was then followed as for the first reaction.

A special experimental procedure was necessary to run the neopentane reactions (Fig. 3). The reaction was first run at 473 K for 3.6 ks (1 h) to hydrogenate the olefins present as impurities. The products of the hydrogenation were *n*-butane (0.1%), *n*-pentane (0.01%), and isopentane (0.03%). After the hydrogenation step, the reaction temperature was increased to the desired level. The low level of the isomerization product (isopentane) formed through hydrogenation had to be subtracted from the total rate, especially when measuring rates on samples with low amounts of platinum on the surface. A sulfur-containing compound was also present as an impurity as evidenced by AES analysis at the end of the reaction when the samples were not sulfided. The accumulation of sulfur after neopentane reactions was observed in our laboratory before (16). The sulfur compound could not be identified by gas chromatography.

On the reaction of cyclohexane dehydrogenation, after the sulfidation step the sample was heated to 800 K in 450 kPa of H_2 for 1 min to remove sulfur bound to platinum. The reason for this treatment was that the lower reaction temperature in this reaction (573 K) might not be sufficient to remove most of the sulfur adsorbed on platinum.

Blank experiments were run to certify that no background catalytic activity was present. Those experiments were run on a sulfided rhenium foil at the same reaction conditions used in the other experiments. On the reactions with *n*-hexane and cyclohexane no reaction products were observed after 1 h and up to the maximum reaction temperature of 800 and 570 K, respectively.

2.3. *Temperature Measurement*

For the calculation of rates, the precise measurement of the reaction temperature has to be certified. When running reactions with a hydrocarbon that can be dehydrogenated to an olefin, the most direct way to certify that the thermocouple spot-welded to the sample is measuring the true reaction temperature is to verify if the temperature calculated based on the equilibrium concentration of a particular olefin matches the thermocouple temperature (16). For a platinum foil, the temperature as calculated from the thermodynamic equilibrium isobutane–isobutene is consistently about 20 K lower than the thermocouple temperature (Fig. 4) until about 740 K when the deviation becomes bigger. Also plotted is the temperature calculated from the *n*-hexane-1-hexene equilibrium on a platinum foil and on a rhenium foil covered with about six monolayers of platinum. In this case the measured temperature on the two different foils is very similar and agrees with the temperature derived from the isobutane–isobutene equilibrium at low temperatures but then deviates more as the temperature is increased. This discrepancy at higher temperatures is due to the deposition of carbon on the catalyst surface and consequent deactivation before equilibrium can be established, as will be dis-

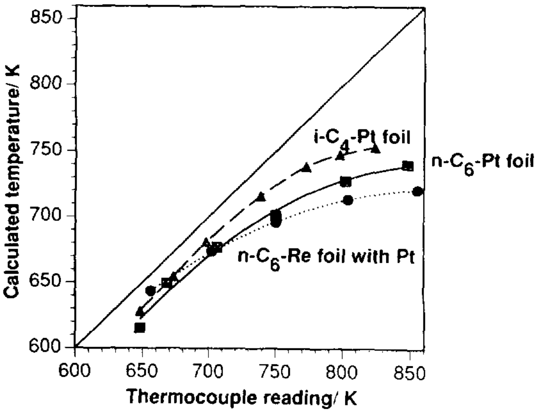

FIG. 4. Calculated temperature based on the thermodynamic equilibrium between isobutane-isobutene on a platinum foil (▲), *n*-hexane-1-hexene on a platinum foil (■), or on a platinum-covered rhenium foil (●). Reaction run with 450 kPa H_2, 13.3 kPa of hydrocarbon.

TABLE 1

Difference between the Temperature of the Thermocouple and the Temperature Calculated from the *n*-Hexane-1-Hexene Equilibrium as a Function of H_2 Pressure

H_2 Pressure/kPa[a]	Temperature difference/K
446	74
963	44
1380	24

[a] Reaction run at 802 K, 13 kPa of *n*-hexane, and variable H_2 pressure.

cussed in more detail throughout this paper. At this point it should only be noted that when the H_2 pressure is increased the temperature deviation becomes smaller (Table 1). Higher H_2 pressure inhibits the formation of carbon deposits and the temperature should be closer to the calculated one. In conclusion, the temperature is reproducible and is about 20 K below the predicted temperature. The temperatures quoted in the paper are the ones measured by the thermocouple.

3. RESULTS AND DISCUSSION

The objective of this paper is to understand why the activity maintenance of platinum–rhenium–sulfur catalysts for hydrocarbon reactions is better than the activity maintenance for platinum catalysts. The approach used in this work is to correlate the activity maintenance with the surface composition. The first task was to measure the amounts of platinum, rhenium, sulfur, and carbon on the surface and show how these parameters affect the overall rate. Next, the activity maintenance for the *n*-hexane and cyclohexane reactions as a function of surface composition was studied.

3.1. Surface Composition of Platinum and Rhenium

To obtain the coverage of platinum on a rhenium foil as a function of deposited platinum, the absolute height of the Auger rhenium 215 eV peak is plotted against the number of platinum pulses (Fig. 1). A linear plot with breaks at regular intervals indicates, according to the model of Frank–Van der Merwe (32), that the deposition occurs layer-by-layer. It also indicates that the metal deposition is uniform. The same kind of plot is obtained by the deposition of rhenium on platinum foil (Fig. 1). These plots are used to estimate the amount of surface metal when the sample is not annealed after deposition. One monolayer is formed after about 15 pulses. An independent way of measuring the coverage is by biasing the sample at a negative voltage (−100 V) and measuring the current collected for each plasma pulse (33). The knowledge of the average charge for the cation in the plasma (+2.1 for Pt) and the area of the sample permits one to calculate the amount of cations arriving at the sample per pulse as 1.7×10^{14} platinum cations cm^{-2} or about 9 pulses per monolayer. This result does not agree with the coverage derived from the Auger electron spectroscopy (AES) measurement. The difference in coverage is expected because the energy of the cations in the plasma have an energy distribution between 50 and 400 eV, and it is expected that a fraction of the cations will penetrate into the foil a few layers deep thus contributing an attenuated signal to the surface Auger signal. The subsurface fraction is about 40% if it is assumed that the value of 15 pulses per monolayer predicted by AES is correct.

To obtain a surface which was as uniform as possible, the samples were annealed after deposition at 1000 K for 1 min, a treatment that caused some of the surface atoms to diffuse into the bulk, as observed before (18). For the case of the deposition of rhenium on a platinum foil, the ratio of the rhenium 215 eV AES peak to the platinum 252 eV peak decreases by a factor of about 3 after annealing when 20 to 100 pulses of rhenium are applied on platinum foils. Due to the atom diffusion into the bulk, some of the Auger electrons might be coming from atoms which are not on the surface. Thus, the amount of platinum on the surface cannot be correlated directly with the AES signal and the amount of platinum on the surface had to be measured in an independent experiment. The isomerization of neopentane to isopentane was chosen as the probe reaction. The isomerization reaction is characteristic of a few noble metals (34) and does not occur to any extent on rhenium. The isomerization can occur by a bond-shift (35) or metallacyclobutane mechanism (36, 37). The number of sites required on a bond-shift mechanism is three (6) and only one based on a metallacyclobutane mechanism (38). If it is assumed that the fraction of neopentane reacting through each mechanism will remain the same as the platinum ensemble sizes are decreased, then the platinum coverage will be given by the ratio of isomerization rates of the covered foil and the pure platinum foil.

The choice of this reaction to count the number of sites was dictated by the fact that the probe reaction could be run at the same conditions as the *n*-hexane reactions. This is important because the sulfur coverage on platinum is a function of the reaction conditions. For example, the hydrogenation of ethene at room temperature is a better choice to measure the number of sites (39), but at room temperature sulfur will cover all the platinum sites and no activity will be detected.

The nominal turnover rate per total surface atom is plotted as a function of the amount of rhenium pulses for a platinum foil (Fig. 5A) and as a function of platinum pulses for a rhenium foil (Fig. 5B). The hydrogenolysis

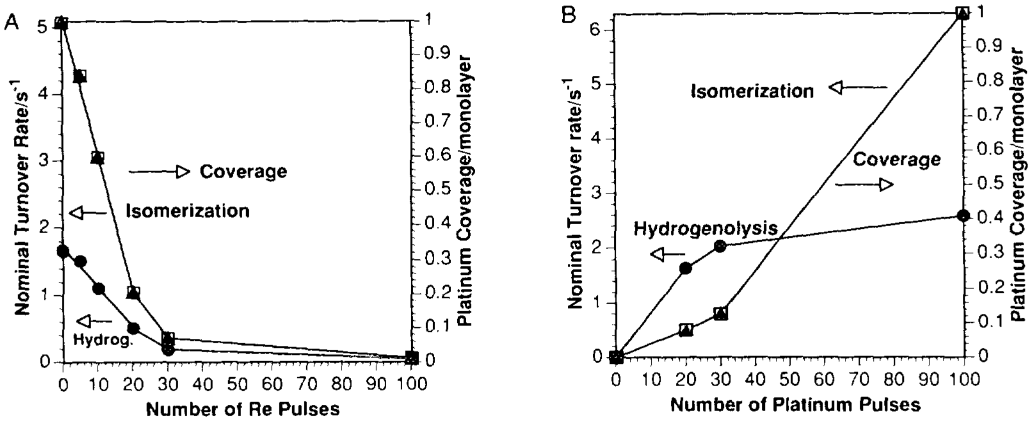

FIG. 5. (A) Nominal turnover rate for the isomerization (☐) and hydrogenolysis (●) of neopentane on a platinum foil as a function of deposited rhenium. The platinum coverage calculated from the isomerization rates is also shown (▲). Reaction run with 13.3 kPa of neopentane, 450 kPa of H_2, and 740 K. (B) Nominal turnover rate for the isomerization (☐) and hydrogenolysis (●) of neopentane on a rhenium foil as a function of deposited platinum. The platinum coverage calculated from the isomerization rates is also shown (▲). Reaction run with 13.3 kPa of neopentane, 450 kPa of H_2, and 740 K.

products were methane, ethane, propane, and isobutane. The rate of hydrogenolysis decreased with the amount of rhenium, but at a lower pace than the isomerization rate. This is to be expected since rhenium also catalyses the hydrogenolysis reaction and some rhenium may be exposed to the reactants by loss of sulfur during reaction. The only isomerization product was isopentane. At 100 pulses of rhenium on a platinum foil or over a rhenium foil the measured rates for isomerization and hydrogenolysis could not be distinguished from the background. This fact shows that sulfided rhenium has virtually no activity in the reactions of neopentane: it just blocks platinum sites.

Because isomerization occurs exclusively on platinum, the ratio of the isomerization rate on rhenium covered platinum to the rate on pure platinum was used to calibrate the platinum surface coverage (Figs. 5A and 5B). This calibration will be used throughout the rest of the paper to calculate the rhenium or platinum surface coverage.

3.2. *Surface Composition of Sulfur and Carbon*

The amount of sulfur and carbon were investigated by AES after two consecutive reactions with 13.3 kPa *n*-hexane, 450 kPa H_2, 740 K, lasting about 5 ks each (Figs. 6A and 6B). The AES ratios are shown for the samples that were presulfided and then run with or without added thiophene. The coverage of sulfur was estimated by the ratio of the S 152 eV peak height to the (Pt + Re 237 eV) peak height. The calibration for the sulfur coverage was determined previously for a sulfur coverage of 1/3 of a monolayer on the structure Pt(111) − $(\sqrt{3} \times \sqrt{3})R30°$-S, with one monolayer corresponding to a ratio of the S 152 eV peak height to the Pt 237 eV peak height of about 30 (40). The amount of sulfur after reaction increases with the amount of rhenium (Fig. 6A). Also, the samples lose most of the sulfur during reaction if no thiophene is added, with the sample with no rhenium or thiophene added losing all the sulfur. A similar result was found for supported catalysts (41). Sulfur is lost probably by the formation of H_2S under the high H_2 pressure (450 kPa) and high temperature (740 K) used in this experiment. If no additional source of sulfur is added, the H_2S that escapes from the surface will probably be adsorbed on the stainless-steel reactor walls and the H_2S gas phase concentration will decrease. Note that the sulfur surface coverage at steady-state conditions will be a function of the ratio of the pressures of H_2S to H_2 and the temperature (42).

Figure 6B shows the ratio of the AES C 272 eV peak height to the (Pt + Re 237 eV) peak height. For the quantification of the amount of carbon on the surface, a previously measured value of C_{272}/Pt_{237} AES peaks for Pt(111) yields a value of 1.5 for a surface coverage of one carbon per platinum surface atom (43). Large amounts of carbon are on the surface after reaction (Fig. 6B). It has been shown before that three-dimensional carbon deposits grow on the surface under high temperature and low H_2 pressure (43). The carbon coverage decreases as rhenium and sulfur are added to the surface, which is an indication of the beneficial effect of rhenium and sulfur in preventing carbon buildup. For a supported catalyst, the amount of carbon deposited is about the same for supported Pt and Pt–Re catalysts (44) but the nature of the carbon on supported catalysts seems to be different (27). The difference in carbon buildup between model and supported catalyst might be related to the availability of a high surface area support for spillover of carbonaceous deposits (39).

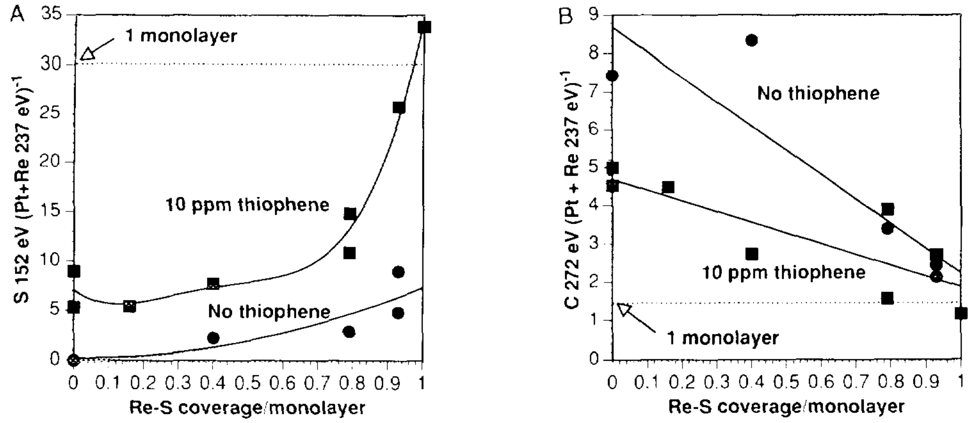

FIG. 6. (A) Ratio of the sulfur 152 eV AES peak to the combined platinum and rhenium peak (Pt + Re 237 eV) as a function of the rhenium–sulfur coverage after two runs at 740 K, 13.3 kPa of *n*-hexane, and 450 kPa of H_2 with (■) and without (●) added thiophene. (B) Ratio of the carbon 272 eV AES peak to the combined platinum and rhenium peak (Pt + Re 237 eV) as a function of the rhenium–sulfur coverage after two runs at 740 K, 13.3 kPa of *n*-hexane, and 450 kPa of H_2 with (■) and without (●) added thiophene.

3.3. Adsorbed Sulfur Makes the Catalyst More Stable

Figure 7A shows a typical accumulation versus time plot for *n*-hexane reactions on a platinum foil catalyst with no rhenium added. Figure 7B shows the reaction under the same conditions when 10 ppm of thiophene is added to the reactant mixture. The initial rates are lower in Fig. 7B but the catalyst shows a lower deactivation rate with an end result of about the same concentration of products at the end of the run as in Fig. 7A. Clearly, the catalyst deactivates less when sulfur is maintained on the surface of platinum. As shown above by AES (Fig. 6A), when rhenium is present the surface can hold sulfur much better. Thus, the platinum–rhenium surfaces should deactivate even less if sulfur has a beneficial effect. Indeed, Fig. 8 shows that on the rhenium containing platinum foil the rate of deactivation is lower than on the platinum samples in Fig. 7 with the same amount of thiophene. In conclusion, sulfur alone can decrease the rate of deactivation and it is easier to maintain the sulfur surface concentration with rhenium.

Note that on the samples with added rhenium, and even with added thiophene, the rate of hydrogenolysis goes up sharply with time. The reason for the increase in the hydrogenolysis rate is that in a batch reactor the amount of thiophene added in the beginning of the reaction is depleted causing the rhenium to lose sulfur under reaction conditions (Fig. 6A). It is then concluded that the plati-

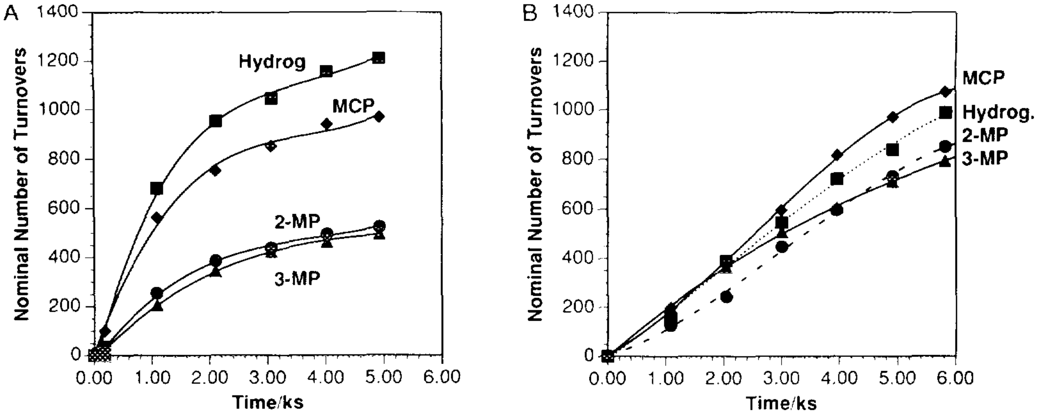

FIG. 7. (A) Number of *n*-hexane molecules converted to hydrogenolysis products (■), 2-methylpentane (●), 3-methylpentane (▲), and methylcyclopentane (◆) per surface platinum atom as a function of time. Reaction run on a sulfided platinum foil at 13.3 kPa of *n*-hexane, 450 kPa of H_2, and 740 K. (B) Number of *n*-hexane molecules converted to hydrogenolysis products (■), 2-methylpentane (●), 3-methylpentane (▲), and methylcyclopentane (◆) per surface platinum atom as a function of time. Reaction run on a sulfided platinum foil at 13.3 kPa of *n*-hexane, 450 kPa of H_2, 10 ppm of thiophene, and 740 K.

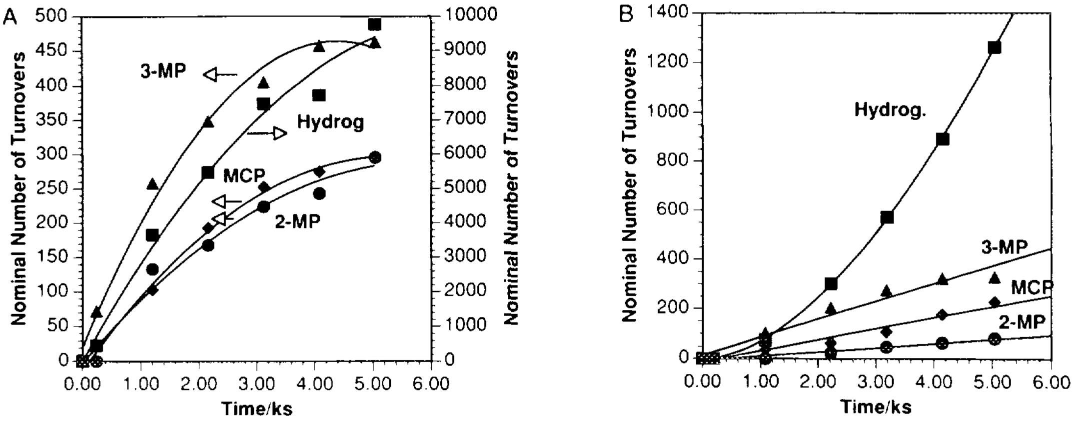

FIG. 8. (A) Number of *n*-hexane molecules converted to hydrogenolysis products (■), 2-methylpentane (●), 3-methylpentane (▲), and methylcyclopentane (◆) per total surface metal atom as a function of time. Reaction run on a sulfided platinum foil with 0.93 ML of rhenium at 13.3 kPa of *n*-hexane, 450 kPa of H_2, and 740 K. (B) Number of *n*-hexane molecules converted to hydrogenolysis products (■), 2-methylpentane (●), 3-methylpentane (▲), and methylcyclopentane (◆) per surface metal atom as a function of time. Reaction run on a sulfided platinum foil with 0.93 ML of rhenium at 13.3 kPa of *n*-hexane, 450 kPa of H_2, 10 ppm of thiophene, and 740 K.

num–rhenium system will be viable as a reforming catalyst (low hydrogenolysis) only if the rhenium remains sulfided under reaction, a condition that is met naturally under industrial conditions since naphthas have small amounts of sulfur compounds.

Also, the stability is lower on a catalyst with less sulfur as shown in Figs. 7A and 7B and Figs. 8A and 8B. Thus, sulfur has to be added to decrease the hydrogenolysis rate and to make the catalyst stable: platinum–rhenium alone will not have a lower deactivation rate. The same conclusion was derived for a supported catalyst (27).

3.4. Variation of Rates with Rhenium-Sulfur Coverage

The variation of nominal turnover rates as a function of the amount of rhenium on the surface is shown in Fig. 9A and 9B for runs with no added thiophene and with 10 ppm of thiophene. The discussion of the data is better accomplished if the reactions of hydrogenolysis and dehydrogenation are discussed separately from the reactions of isomerization and cyclization.

The hydrogenolysis reactions are catalyzed by both platinum and rhenium. There is a maximum in the nominal turnover rate of hydrogenolysis as the amount of rhenium

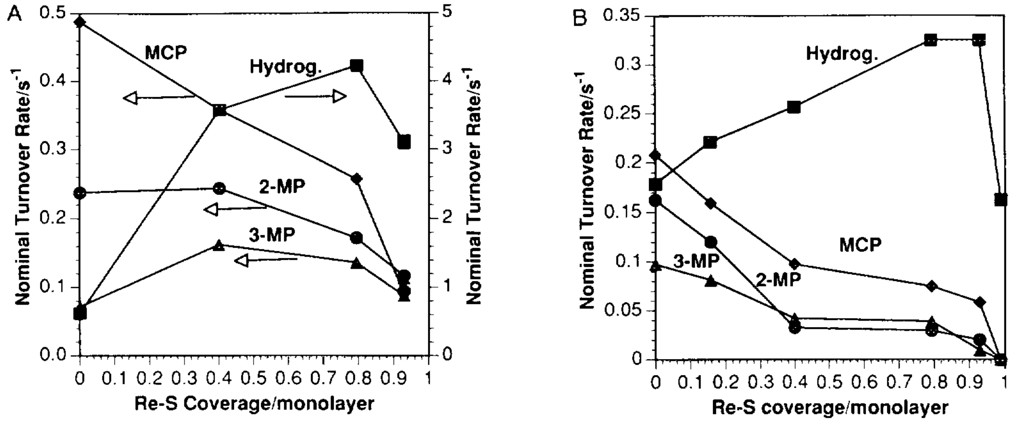

FIG. 9. (A) Number of *n*-hexane molecules converted per surface metal atom per second to hydrogenolysis products (■), 2-methylpentane (●), 3-methylpentane (▲), and methylcyclopentane (◆) as a function of rhenium–sulfur coverage. Reaction run on a sulfided platinum foil at 13.3 kPa of *n*-hexane, 450 kPa of H_2, and 740 K. (B) Number of *n*-hexane molecules converted per surface metal atom per second to hydrogenolysis products (■), 2-methylpentane (●), 3-methylpentane (▲), and methylcyclopentane (◆) as a function of rhenium–sulfur coverage. Reaction run on a sulfided platinum foil at 13.3 kPa of *n*-hexane, 450 kPa of H_2, 10 ppm of thiophene, and 740 K.

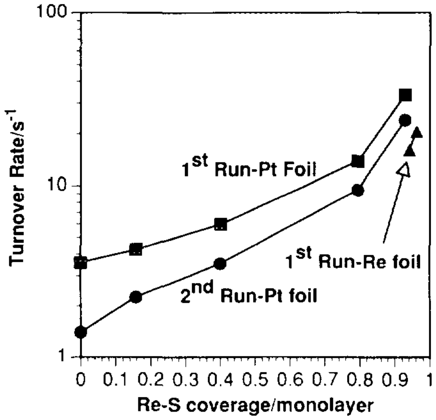

FIG. 10. Turnover rate for *n*-hexane molecules converted to 1-hexene. First run (■), and second run (●) on a sulfided platinum foil as a function of deposited rhenium and first run on a sulfided rhenium foil as a function of deposited platinum (▲). Reaction run at 13.3 kPa of *n*-hexane, 450 kPa of H_2, 10 ppm of thiophene, and 740 K.

on the surface is increased for runs with and without thiophene (Fig. 9). The effect is not so pronounced in the case of samples with added thiophene because these samples can keep a higher amount of sulfur on the surface which blocks the platinum–rhenium sites responsible for hydrogenolysis. The cause for the maximum observed here is probably the same as for the case of *n*-butane hydrogenolysis on Pt–Re catalysts (45): the maximum in the rate was proposed to be due to a variation in the rate determining step from carbon–carbon fission (for a platinum-rich system) to desorption of methane (for rhenium-rich systems) as the relative concentration of platinum and rhenium on the surface were varied. A maximum in the rate was observed before for the cyclopentane and butane hydrogenolysis (22), ethane hydrogenolysis (19), and *n*-hexane reactions at lower pressures (17). It is concluded that rhenium is responsible for the higher rate of hydrogenolysis.

The nominal turnover rates of isomerization and cyclization decrease with the amount of rhenium on the surface. This is expected since these reactions are catalyzed only by platinum and the amount of sites with the minimum ensemble size necessary to catalyze the reaction will decrease as the amount of platinum is decreased. The rates will eventually decrease to zero when the surface is almost completely covered with rhenium (Fig. 9B). When thiophene is added there is also a decrease in the rates and they are lower than for the corresponding samples without thiophene (Fig. 9A). The lower rates when thiophene is added is probably due to the blockage of some of the platinum sites by adsorbed sulfur, a well-known poison.

The dehydrogenation reactions are perhaps the most interesting reactions to be followed. The hydrogenation–dehydrogenation function is the only one that needs to be maintained for the reforming reactions to take place in a bifunctional mode on an industrial catalyst. The initial turnover rate for the dehydrogenation of *n*-hexane to 1-hexene on platinum and rhenium foils is plotted in Fig. 10 as a function of the rhenium coverage. For the calculation of the turnover rates, the total number of platinum atoms on the surface was measured by the neopentane reactions (Fig. 5). Because this reaction reaches equilibrium quickly, a second reaction run was carried out after the first run to probe the amount of deactivation. Two trends are observed in Fig. 10 that point to a better catalyst stability. The first is that the turnover rate increases as the amount of rhenium on the surface is increased. Since this is a structure insensitive reaction the turnover rate should be the same as the surface concentration of rhenium is varied. This result suggests that the rates measured are not initial, but are the rates on a surface heavily and quickly poisoned. As the amount of rhenium is increased, rates closer to initial rates can be measured. The second observation is that the amount of deactivation as measured by the ratio of the initial rate on the second run to the initial rate on the first run also decreases as the amount of rhenium is increased. The results on a rhenium and platinum foil are also in good agreement. These results point to the fact that the lower rate of deactivation seems to be related to the partition of platinum ensembles. If this size effect is correct, an even better way to prepare highly dilute platinum ensembles is to deposit small amounts of platinum on top of a rhenium foil (Fig. 11). The accumulation plot for the dehydrogenation of hexane to 1-hexene on three samples with small amounts of platinum is shown in Fig. 11. The equilibrium value of 1-

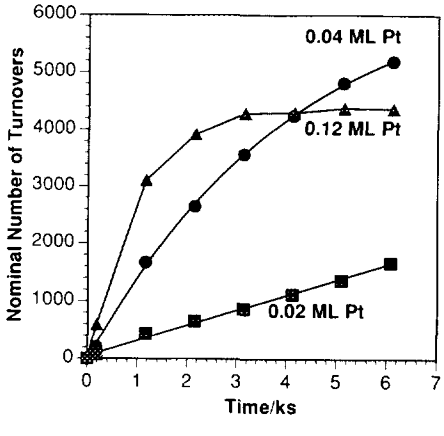

FIG. 11. Number of *n*-hexane molecules converted to 1-hexene per surface atom as a function of time. Reaction run on a sulfided rhenium foil with 2 × 10^{-2} ML (■), 4 × 10^{-2} ML (●), and 1.2 × 10^{-1} ML (▲) of platinum at 13.3 kPa of *n*-hexane, 450 kPa of H_2, 10 ppm of thiophene, and 770 K.

hexene corresponds to a nominal number of turnovers equal to 16,000. Thus, at the end of the runs the concentration of 1-hexene is far from the equilibrium value. The catalyst with the largest amount of platinum (0.12 ML) deactivates before equilibrium can be reached. The catalyst with the intermediate amount of platinum (0.04 ML) deactivates less, the 1-hexene concentration surpasses the concentration obtained with the 0.12-ML sample but it still deactivates as shown by the curvature in the plot. This curvature is not due to the approach to equilibrium since 1-hexene added at the beginning of the reaction at this concentration does not affect the rates. The catalyst with the lowest amount of platinum (0.02 ML) does not deactivate as shown by the straight line plot. Again, the catalyst is more stable as the size of the platinum ensembles on the surface are decreased.

The reactions with *n*-hexane were difficult to follow because under reaction conditions the dehydrogenation reactions quickly reach equilibrium if a low temperature is used or deactivate before an initial rate can be measured if a high temperature is used. Cyclohexane has a higher turnover rate of dehydrogenation than *n*-hexane and reaches an equilibrium concentration about seven times higher for the same hydrogen to hydrocarbon ratio used in the *n*-hexane reaction at 573 K. Thus, initial rates could be easily measured (Fig. 12).

The accumulation versus time plots (Fig. 12) show some interesting trends. The first one is that the rate decreases as time increases for all the samples except for the samples with low coverages (low ensemble size) of platinum. The rate decrease is not due to product inhibition since the same curve shape can be found by adding 1.2% benzene at the beginning of the reaction (the maximum concentration of benzene in Fig. 12 is about 1%). It was also found that the initial rate found by rerunning the reaction a second time was equal to the final rate on the first run. Those two observations indicate that the decrease in the rates during reaction is due to catalyst deactivation.

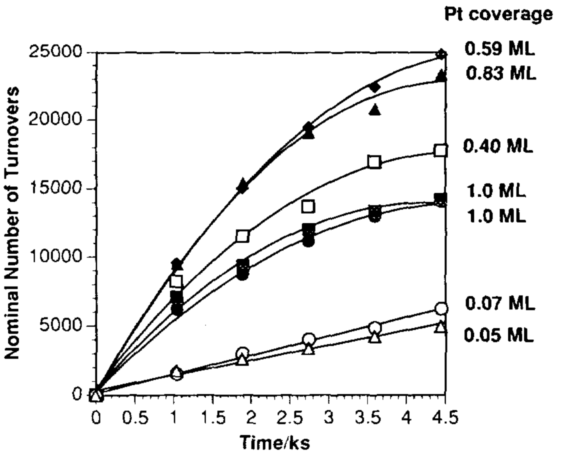

FIG. 12. Number of cyclohexane molecules converted to benzene per surface atom as a function of time. Reaction run on a sulfided platinum foil with different amounts of deposited rhenium at 6.7 kPa of cyclohexane, 450 kPa of H_2, and 573 K. The platinum coverages were 1.0 ML (■), 1.0 ML (●), 0.83 ML (▲), 0.59 ML (◆), 0.40 ML (□), 0.07 ML (○), and 0.05 ML (△).

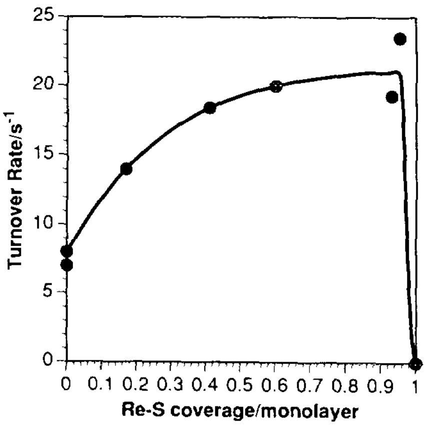

FIG. 13. Turnover rate for the dehydrogenation of cyclohexane to benzene. Reaction run on a sulfided platinum foil with different amounts of deposited rhenium at 6.7 kPa of cyclohexane, 450 kPa of H_2, and 573 K. The number of surface platinum atoms were counted by the reaction of neopentane.

Another feature in Fig. 12 is that the nominal turnover rate (slope of the curves at time zero) initially increases with the amount of Re being added. This rate increase points out to the beneficial effect on Re on the rates: even though the amount of Pt is decreasing, the nominal rate is increasing. As more rhenium is added and the amount of Pt is decreased, the nominal turnover rate eventually decreases. Note, however, that the initial turnover rate, calculated by counting the platinum surface atoms with the neopentane reactions, increases as the size of the ensembles are decreased and then levels off (Fig. 13). The higher than expected rate on the last point is probably due to experimental error because the amount of surface platinum was measured by extrapolation on Fig. 5A in this case. This result establishes that large ensembles of platinum will deactivate quickly to a point where an initial rate cannot be measured.

In the cyclohexane dehydrogenation the reaction conditions are much less drastic than the ones used for the reaction of *n*-hexane and the turnover rate actually levels off after the platinum ensembles get small enough. For the dehydrogenation of *n*-hexane, the leveling off did not occur (Fig. 10) because the reaction conditions are too drastic (the H_2 pressure is not high enough for the temperature used) and the catalyst gets heavily poisoned before an initial rate can be measured. The drastic conditions for the *n*-hexane reactions had to be used to produce a difference among the various rhenium coverage catalysts.

3.5. *Comparison of Rates with Literature Values*

The reactions of hydrogenolysis, dehydrocyclization, cyclization, and isomerization of *n*-hexane are structure-sensitive. The structure of the foil was not uniform and thus comparison of the rates with other catalysts was not attempted. However, the dehydrogenation reactions are structure-insensitive and a comparison with published rates is possible. For the dehydrogenation of *n*-hexane the catalyst deactivates so fast that an initial rate could not be measured (Fig. 10). Also, the dehydrogenation rates are usually not reported in the literature because it is difficult to measure rates on a reaction which is so fast and that at the same time has a very low product equilibrium concentration. The rate of cyclohexane dehydrogenation can be measured more easily. Assuming that the reaction order is zero on H_2 and cyclohexane pressure, as in the case of methylcyclohexane dehydrogenation on platinum (46), the turnover rates reported in the literature (47) at 573 K ($1-15\ s^{-1}$) are about the same as the ones reported in Fig. 13.

The dehydrocyclization of *n*-hexane to form benzene, reported before in purely metallic supported (7) and single crystals (48, 49), was not found in this work. The explanation for the difference in the model system is that the previous work was done at a much lower H_2 pressure (48, 49), which favors the formation of aromatics through gas-phase reactions of hexatrienes (7). The explanation for the difference in selectivity obtained at a higher pressure may be due to the fact that the dehydrocyclization of *n*-hexane to benzene is the first reaction to be poisoned by carbonaceous buildup (50), and poisoning is especially drastic in this model system.

3.6. *Why the Model Catalyst Deactivates So Fast*

For reforming reactions on supported catalysts the catalyst life is strongly dependent on the H_2 partial pressure. According to Sinfelt (51) below about 600 kPa of H_2 and at about 740–800 K, background reactions with extensive formation of carbonaceous deposits become important. A stabilizing factor on an industrial catalyst is probably the large surface area provided by the support, which extends the catalyst life by spillover of carbonaceous deposits from the metal onto the support (39). Also, deactivation is a structure-sensitive reaction. It was shown that flat surfaces like Pt(111) will deactivate more quickly than a kinked one such as Pt(654) (52). A foil is polycrystalline but shows preferentially (111) sites while a supported catalyst composed of small particles has sites of low coordination like the ones on a kinked surface. In fact, as the metal particles become smaller on a supported catalyst, showing more unsaturated sites, the rate of deactivation decreases (53). Thus, poisoning on *n*-hexane reactions on the model systems at the conditions run in this study is expected to be much more severe than for supported catalysts. This deactivation can be so severe that the equilibrium concentration of olefins, quickly equilibrated on a supported catalyst, is not established (Fig. 4). The higher temperature deviation at a higher reaction temperature shown in Fig. 4 is a consequence of the quicker rate at which the surface is poisoned as the temperature is increased. The increase in the curvature in the graphs in Fig. 4 as the temperature approaches about 740 K is corroborated by the break in the Arrhenius plot for hexane dehydrogenation around that temperature for a platinum foil (Fig. 14). The same curvature in the Arrhenius plot was observed before at lower temperatures but lower H_2 pressures (49). Also, as the catalyst is made more resistant to carbon deposition by the dilution of platinum, there is no break in the Arrhenius plot (Fig. 14) and the difference between the calculated and measured temperatures becomes smaller. For example, at 740 K, on a platinum foil, for the reaction of *n*-hexane, the temperature difference between the thermocouple temperature and the calculated temperature from the olefin concentration is about 70 K with no sulfur or thiophene added, about 40 K when the surface is presulfided and thiophene is added, and on a presulfided rhenium foil with 4×10^{-2} ML of platinum with added thiophene it is 15 K, or equal to the error expected. Again, Fig. 14 illustrates the main point of this paper that small ensembles of platinum separated by sulfur atoms will be more resistant to deactivation.

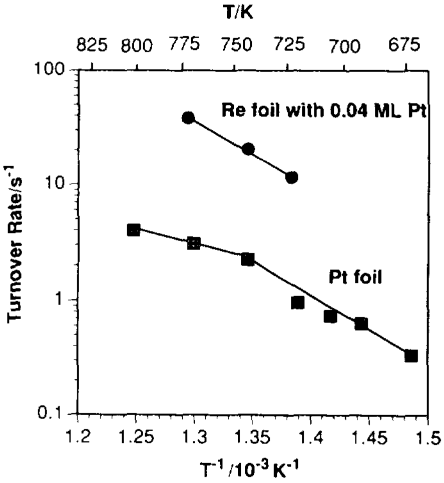

FIG. 14. Arrhenius plot for the dehydrogenation of *n*-hexane to 1-hexene on a sulfided platinum foil (■) and on a sulfided rhenium foil with 4×10^{-2} ML of platinum (●). Reaction run at 13.3 kPa of *n*-hexane and 450 kPa of H_2.

3.7. *A Description of the Working Catalyst*

It was shown above that the catalysts that resist poisoning best are those for which the number of platinum–platinum neighbors on the surface are very small. The question that needs to be answered is why this arrangement produces a much more stable catalyst. Earlier proposals suggest that the sulfur atoms that protrude out of the surface will create a steric hindrance so that carbonaceous fragments will not have a chance to meet and form large, highly dehydrogenated species (23, 24). This model assumes that the sulfur atoms are immobile and adsorbed over rhenium. The surface immobility is reasonable in view of the results that the hydrogenolysis activity of platinum–rhenium systems is very high but is drastically reduced when sulfur is adsorbed, which can be rationalized only if the sulfur is immobile over rhenium. The importance of sulfur was also demonstrated in this work in that the catalytic stability was derived only if rhenium was added with sulfur, which shows that just diluting platinum is not sufficient. In conclusion, if the above model is correct, then it is expected that any other element that forms strong bonds with sulfur and alloys with platinum (e.g., tungsten) should work as well.

There are some other platinum alloy catalysts that are used in industry for their higher stability (Pt–Ir, Pt–Sn). In the case of Pt–Ir the same mechanism as proposed here for Pt–Re might be operating, with sulfur forming strong bonds to iridium. However, the case of Pt–Sn might be different because tin is an inert element and will not form bonds to sulfur. In Pt–Re–S the sulfur atoms will protrude out of the surface and in Pt–Sn the tin atoms will be alloyed with platinum probably forming a "smooth" surface. It remains to be investigated if this is an important difference.

The optimal composition of the Pt–Re catalyst will be a function of the desired catalytic properties. If the function of platinum is just to catalyze hydrogenation–dehydrogenation reactions, then the amount of rhenium should be maximized since it produces the most stable catalysts. However, if a functionality other than hydrogenation–dehydrogenation is to be kept on the platinum (isomerization, cyclization), larger ensemble sizes are necessary and they cannot be reduced drastically.

Finally, it should be mentioned that although Pt–Re–S is a superior catalyst as compared to Pt–S; in an industrial catalyst the metallic function is supported on alumina. The possibility that rhenium interacts with the alumina and modifies the support or platinum leading to an improved catalyst performance was not tested in this study.

4. CONCLUSIONS

Rhenium is a very good hydrogenolysis catalyst, especially when alloyed with platinum. This higher hydrogenolysis activity is not the cause for enhanced catalyst stability. The hydrogenolysis activity can be removed by sulfidation of the catalyst, which caps the rhenium with sulfur. The rhenium–sulfur compound has no catalytic activity on hydrocarbon reactions and acts only as a diluent for platinum.

Increased resistance to deactivation appears when sulfur is added to platinum. However, a platinum catalyst quickly loses its adsorbed sulfur except when rhenium is also present.

The Pt–Re–S system shows different product selectivity than Pt–S because the ensemble sizes of platinum are modified and because rhenium retains sulfur on the surface much better than platinum. Reactions that require large ensembles (hydrogenolysis, dehydrocyclization, isomerization, and cyclization) will decrease as the platinum ensembles are reduced. However, the turnover rates on hydrogenation–dehydrogenation reactions are not affected by the size of the ensemble and thus, as expected, alloying with rhenium did not affect the initial turnover rate (when severe deactivation can be excluded).

The small ensembles of platinum that were prepared by dilution with rhenium–sulfur were very stable against poisoning by carbon deposition. This stabilization effect comes as a consequence of the small platinum ensemble sizes which cannot build up carbonaceous deposits because there is no space for a large polymeric carbon structure to grow. Thus, this catalyst is very stable until the adjacent platinum–rhenium–sulfur moieties lose their sulfur and expose large patches of platinum–rhenium where polymeric carbon structures may grow.

ACKNOWLEDGMENTS

This work was supported by the Director, Office of Energy Research, Office of Basic Energy Sciences, Materials Sciences Division, of the U.S. Department of Energy under Contract DE-AC03-76SF00098. A. L. Bonivardi acknowledges financial support from the Consejo Nacional de Investigaciones Científicas y Técnicas of the República Argentina. We thank Drs. Ian G. Brown, Andres, and Simone Anders for their help with the plasma gun, and Dr. John H. Sinfelt and Professor Calvin H. Bartholomew for their insightful comments on the final version of the paper.

REFERENCES

1. Gates, B. C., Katzer, J. R., and Schuit, G. C. A., *in* "Chemistry of Catalytic Processes," McGraw–Hill, New York, 1979.
2. Boudart, M., and Djéga-Mariadassou, G., *in* "Kinetics of Heterogeneous Catalytic Reactions." Princeton Univ. Press, Princeton, NJ, 1984.
3. Mills, G. A., Heinemann, H., Milliken, T. H., and Oblad, A. G., *Ind. Eng. Chem.* **45,** 134 (1953).
4. Illes, V., and Schindlbauer, H., *Acta Chim. Acad. Sci. Hung.* **82,** 449 (1974).
5. Weisz, P. B., *in* "Actes du Deuxieme Congres International de Catalyse," p. 937. Editions Technip, Paris, 1961.
6. Anderson, J. R., and Avery, N. R., *J. Catal.* **5,** 446 (1966).
7. Dautzenberg, F. M., and Platteeuw, J. C., *J. Catal.* **19,** 41 (1970).
8. Biloen, P., Dautzenberg, F. M., and Sachtler, W. M. H., *J. Catal.* **50,** 77 (1977).

9. Heinemann, H., *in* "Catalysis Science and Technology" (J. R. Anderson and M. Boudart, Eds.), Vol. 1, p. 1. Springer-Verlag, New York/Berlin, 1981.
10. Sinfelt, J. H., *in* "Bimetallic Catalysts: Discoveries, Concepts, and Applications." Wiley, New York, 1983.
11. Butt, J. B., and Petersen, E. E., *in* "Activation, Deactivation, and Poisoning of Catalysts." Academic Press, New York, 1988.
12. Kluksdahl, H. E., U.S. Patent 3,415,737, 1968.
13. Fung, A. S., McDevitt, M. R., Tooley, P. A., Kelley, M. J., Koningsberger, D. C., and Gates, B. C., *J. Catal.* **140,** 190 (1993).
14. Somorjai, G. A., *Catal. Lett.* **15,** 25 (1992).
15. Somorjai, G. A., *in* "Introduction to Surface Chemistry and Catalysis." Wiley, New York, 1994.
16. Davis, S. M., Zaera, F., and Somorjai, G. A., *J. Am. Chem. Soc.* **104,** 7453 (1982).
17. Kim, C., and Somorjai, G. A., *J. Catal.* **134,** 179 (1992).
18. Godbey, D. J., and Somorjai, G. A., *Surf. Sci.* **202,** 204 (1988).
19. Godbey, D. J., Garin, F., and Somorjai, G. A., *J. Catal.* **117,** 144 (1989).
20. Yermakov, Yu. U., and Kuznetsov, B. N., *J. Mol. Catal.* **9,** 13 (1980).
21. Bertolacini, R. J., and Pellet, R. J., *in* "Catalyst Deactivation" (B. Delmon and G. F. Froment, Eds.), p. 73. Elsevier, Amsterdam, 1980.
22. Betizeau, C., Leclercq, G., Maurel, R., Bolivar, C., Charcosset, H., Frety, R., and Maurel, R., *J. Catal.* **45,** 179 (1976).
23. Biloen, P., Helle, J. N., Verbeek, H., Dautzenberg, F. M., and Sachtler, W. M. H., *J. Catal.* **63,** 112 (1980).
24. Sachtler, W. M. H., *J. Mol. Catal.* **25,** 1 (1984).
25. Shum, V. K., Butt, J. B., and Sachtler, W. M. H., *J. Catal.* **96,** 371 (1985).
26. Shum, V. K., Butt, J. B., and Sachtler, W. M. H., *J. Catal.* **99,** 126 (1986).
27. Augustine, S. M., Alameddin, G. N., and Sachtler, W. M. H., *J. Catal.* **115,** 217 (1989).
28. Ponec, V., *Catal. Today* **10,** 251 (1991).
29. Kim, C., Ogletree, D. F., Salmeron, M. B., Godechot, Y., Somorjai, G. A., and Brown, I. G., *Appl. Surf. Sci.* **59,** 261 (1992).
30. Heegemann, W., Meoster, K. H., Betchtold, E., and Hayek, K., *Surf. Sci.* **49,** 161 (1975).
31. Palmberg, P. W., Riach, G. E., Weber, R. E., and MacDonald, N. C., *in* "Handbook of Auger Electron Spectroscopy." Physical Electronics Industries, Edina, Minnesota, 1972.
32. Bauer, E., *Appl. Surf. Sci.* **11/12,** 479 (1982).
33. Chen, F. F., *in* "Plasma Diagnostics Techniques" (R. H. Huddelstone and S. L. Leonard, Eds.), Academic Press, New York, 1965.
34. Boudart, M., and Ptak, L. D., *J. Catal.* **16,** 90 (1970).
35. Anderson, J. R., *in* "Advances in Catalysis" (D. D. Eley, H. Pines, and P. B. Weisz, Eds.), Vol. 23, p. 1. Academic Press, San Diego, 1973.
36. Parshall, G. W., Thorn, D. L., and Tulip, T. H., *Chemtech* **12,** 571 (1982).
37. Garin, F., and Gault, F. G., *J. Am. Chem. Soc.* **97,** 4466 (1975).
38. Foger, K., and Anderson, J. R., *J. Catal.* **61,** 140 (1980).
39. Rivera-Latas, F. J., Dalla Betta, R. A., and Boudart, M., *AIChE. J.* **38,** 771 (1992).
40. Kim, Changmin, Ph.D. Thesis, University of California at Berkeley, 1992.
41. Pönitzsch, L., Wilde, M., Tétényi, P., Dobrovolszky, M., and Paál, Z., *Appl. Catal.* **86,** 115 (1992).
42. Wise, H., and Oudar, J., *in* "Material Concepts in Surface Reactivity and Catalysis," p. 49. Academic Press, New York, 1990.
43. Davis, S. M., Zaera, F., and Somorjai, G. A., *J. Catal.* **77,** 439 (1982).
44. Carter, J. L., McVicker, G. B., Weissman, W., Kmak, W. S., and Sinfelt, J. H., *Appl. Catal.* **3,** 327 (1982).
45. Haining, I. H. B., Kembal, C., and Whan, D. A., *J. Chem. Res. (Microfiche)* 2056 (1977).
46. Sinfelt, J. H., Hurwitz, H., and Shulman, R. A., *J. Phys. Chem.* **64,** 1559 (1960).
47. Somorjai, G. A., *in* "Chemistry in Two Dimensions: Surfaces," p. 456. Cornell Univ. Press, Ithaca, New York, 1981.
48. Sachtler, J. W. A., and Somorjai, G. A., *J. Catal.* **81,** 77 (1983).
49. Davis, S. M., Zaera, F., and Somorjai, G. A., *J. Catal.* **85,** 206 (1984).
50. Iglesia, E., and Baumgartner, J. E., *in* "Proceedings, 10th International Congress on Catalysis, Budapest, 1992" (L. Guczi, F. Solymosi, and P. Tétényi, Eds.) p. 993. Elsevier, Amsterdam, 1993.
51. Sinfelt, J. H., *in* "Catalysis Science and Technology" (J. R. Anderson and M. Boudart, Eds.), Vol. 1, p. 269. Springer-Verlag, New York/Berlin, 1981.
52. Davis, S. M., and Somorjai, G. A., *J. Catal.* **65,** 78 (1980).
53. Lankhorst, P. P., de Jongste, H. C., and Ponec, V., *in* "Catalyst Deactivation" (B. Delmon and G. F. Froment, Eds.), p. 43. Elsevier, Amsterdam, 1980.